

## Magnetic Properties of the Granular Alloy $\text{Fe}_{10}\text{Ag}_{90}$ as a Function of Annealing Temperature

João Maria Soares<sup>a\*</sup>, José Humberto de Araújo<sup>b</sup>, Francisco de Assis Olímpio Cabral<sup>b</sup>,

Thomas Dumelow<sup>c</sup>, Milton Morais Xavier Júnior<sup>c</sup>, José Marcos Sasaki<sup>d</sup>

<sup>a</sup>Departamento de Física, Universidade Federal de Pernambuco, 50670-901 Recife - PE, Brazil

<sup>b</sup>Departamento de Física Teórica e Experimental,

Universidade Federal do Rio Grande do Norte, 59072-970 Natal - RN, Brazil

<sup>c</sup>Departamento de Física, Universidade do Estado do Rio Grande do Norte,  
59633-010 Mossoró - RN, Brazil

<sup>d</sup>Departamento de Física, Universidade Federal do Ceará, 60455-760 Fortaleza - CE, Brazil

Received: November 1, 2004; Revised: May 25, 2005

$\text{Fe}_{10}\text{Ag}_{90}$  granular alloys have been prepared using a sol-gel process, sintered at 300 °C and annealed at temperatures between 400 °C and 700 °C. The mean size of the iron particles, obtained from X-ray diffraction, is  $30.0 \pm 0.7$  nm. Due to the existence of a distribution of particle sizes in these samples, both blocked (BL) and superparamagnetic (SPM) particles are present simultaneously, as confirmed by magnetization measurements at room temperature. AC susceptibility measurements as a function of temperature reveal a magnetic phase transition at about 770 °C, indicating the presence of particles exhibiting bulk behavior, in the samples annealed above 550 °C. The presence of these particles has been attributed to an atomic diffusion process between the grains, forming bulk-like multiple-domain Fe particles having Curie temperatures near that of bulk  $\alpha$ -Fe phase ( $T_C = 770$  °C).

**Keywords:** superparamagnetism, granular alloy, size distribution

### 1. Introduction

The synthesis of nanometer-scale materials has been the focus of intense study in materials science and solid-state chemistry<sup>1,2</sup>. Nano-sized particles of noble metals have attracted considerable interest in various fields of chemistry and physics because of their conspicuous physiochemical catalytic properties and their potential applications in microelectronics, optical, electronic, and magnetic devices<sup>3-6</sup>. Much attention have been paid to granular iron solids because of their interesting physical properties, in particular, the discovery of giant magnetoresistance (GMR)<sup>7,8</sup> and giant magnetoimpedance (GMI)<sup>9</sup>, as well as their application in magnetic recording and optical devices and in sensors<sup>10-12</sup>.

Nanocrystalline Fe particles containing a single magnetic domain exhibit very different magnetic properties from those of bulk Fe. New applications require materials that combine high magnetization and coercivity of single domain Fe particles with a highly conducting matrix. Iron can form alloys or solid solutions with almost all metals, there being few metallic elements with which Fe is immiscible. Ag is an example of such a metal. However, in recent years, it has been shown that metastable and homogeneous alloys of Fe-Ag system can be formed by using special techniques, such as thermal evaporation<sup>13,14</sup>, liquid quenching<sup>15</sup>, ion implantation<sup>16</sup>, sputtering<sup>17-21</sup>, mechanical alloying<sup>22-24</sup>, gas condensation<sup>25</sup> and a sol-gel process<sup>26-28</sup>. FeAg granular alloy, however, is metastable, and upon recrystallization at elevated temperatures, a transformation into separated phases of BCC Fe and FCC Ag occurs.

In this work a series of  $\text{Fe}_{10}\text{Ag}_{90}$  granular alloys has been produced by a sol-gel method and characterized by X-ray diffraction and magnetization measurements. We have observed that in all samples there are particle size distributions composed of SPM and BL particles. A

method for fitting the magnetization curve to a size distribution with these two components has been applied to determine their relative amounts<sup>29</sup>. The changes in annealing temperature  $T_{\text{ann}}$  have a strong influence in the coercive field. The presence of particles exhibiting bulk behavior has been observed by AC susceptibility measurements in the samples annealed above 550 °C.

### 2. Experimental

$\text{Fe}_{10}\text{Ag}_{90}$  granular alloys were produced by a sol-gel process<sup>26-28</sup>. The start solution was prepared from an aqueous solution of Fe and Ag nitrates and nitric acid. The precursor powder obtained was reduced in a hydrogen atmosphere for 45 minutes at a temperature of 400 °C. The resultant powder was pressed and sintered at 300 °C for 8 hours. After sintering, the samples were thermally treated in the temperature range of 400-700 °C.

The crystalline structure of the samples was investigated by conventional X-ray powder diffraction using a Rigaku diffractometer operated with a Mo- $K_{\alpha}$  radiation tube.

The magnetization and hysteresis curves were measured in a vibrating sample magnetometer (VSM) with a maximum magnetic field of 1 T. AC susceptibility was measured in a mutual inductance bridge as described previously<sup>30</sup>.

### 3. Results and Discussion

Figure 1 shows the X-ray patterns of powdered  $\text{Fe}_{10}\text{Ag}_{90}$  granular alloy reduced at a temperature of 400 °C, sintered at 300 °C and annealed at  $T_{\text{ann}} = 700$  °C. It is seen that the iron in  $\text{Fe}_{10}\text{Ag}_{90}$  has a b.c.c. structure and the silver has an f.c.c. structure; there are also some low

\*e-mail: jsoares@df.ufpe.br

intensity reflections from Fe<sub>3</sub>O<sub>4</sub>. Assuming that the Fe in the sample is indeed distributed as small particles, the average particle diameter should be related to the Fe Bragg peak widths by Scherrer's formula. Figure 2 shows part of the diffraction pattern shown in Figure 1 in the interval of 34.4-35.6 (2θ) for samples annealed at 400, 450, 500, 550, 600 and 700 °C. The Bragg peaks for Ag(222) and Fe(211) were fitted

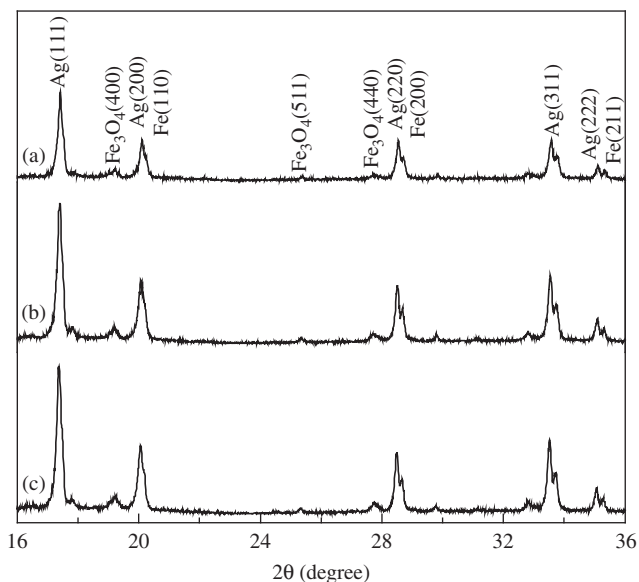


**Figure 1.** X-ray powder patterns of Fe<sub>10</sub>Ag<sub>90</sub> granular alloy. a) Powder; b) Sintered at 300 °C; and c) Sintered at 300 °C and annealed at  $T_{ann} = 700$  °C.

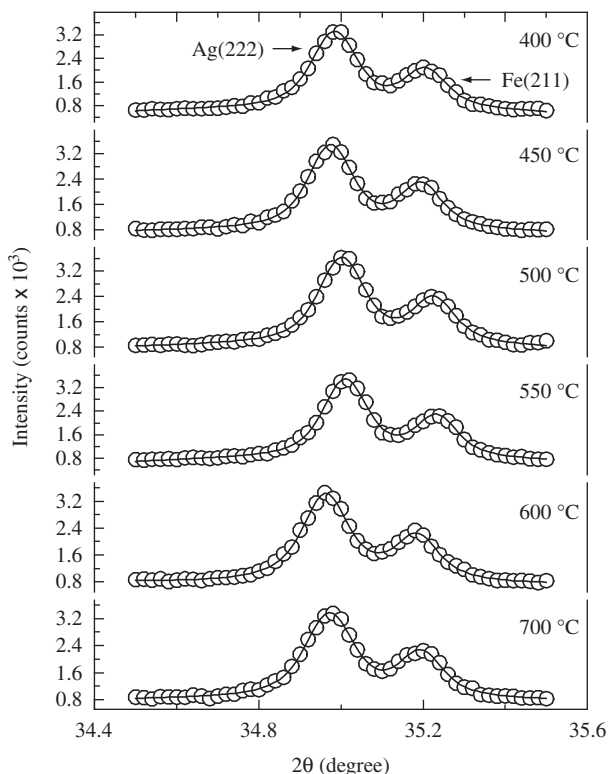


**Figure 2.** X-ray powder patterns of the Ag(222) and Fe(211) peaks of Fe<sub>10</sub>Ag<sub>90</sub> granular alloy, at different annealing temperatures. The solid lines are the fittings obtained using two Pseudo-Voigt functions.

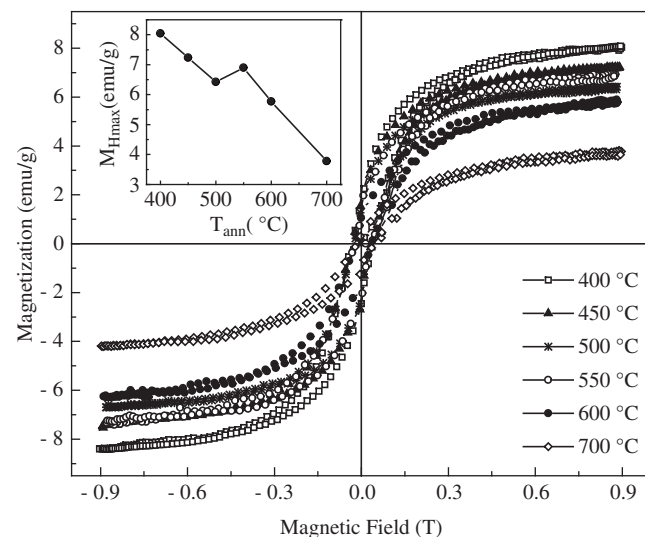
with a pseudo-Voigt function in order to determine the line width. Applying Scherrer's formula, we obtain the average Fe particle sizes  $D_m$  from the (211) line width for different annealing temperatures, as shown in Table 1.  $D_m$  increases from 28.6 nm (powder) to 30 nm (sintered sample). However,  $D_m$  is only slightly affected by  $T_{ann}$ , staying in around 30 nm for all thermal treatment temperatures.

Figure 3 shows the hysteresis curves at room temperature obtained for Fe<sub>10</sub>Ag<sub>90</sub> granular alloy samples annealed at different temperatures. The coercive field, determined from the hysteresis curves, ranges from 365 to 295 Oe, and is two orders of magnitude greater than that of bulk iron, showing the presence of blocked single-domain particles. These curves do not saturate in fields of up to 1 T, indicating the additional contribution of SPM particles. The figure insert shows the maximum field magnetization  $M_{Hmax}$  as a function of the annealing temperature, and it can be seen that  $M_{Hmax}$  decreases linearly with increasing  $T_{ann}$ , up to  $T_{ann} = 500$  °C. However, there is an inflexion at  $T_{ann} = 550$  °C, after which  $M_{Hmax}$  once again decreases linearly with  $T_{ann}$ , but more rapidly. The inflexion at  $T_{ann} = 550$  °C suggests the formation of a different type of particle at this temperature. These particles appear to be larger than the blocked particles, and have multi-domain properties similar to bulk Fe. We attribute their presence to an atomic diffusion process between the grains. Above the inflexion, the proportion and size of large particles increases, and  $M_{Hmax}$  therefore reduces quickly with  $T_{ann}$ . This explanation is supported by AC susceptibility measurements as a function of temperature, as shown in Figure 4. It can be seen that at  $T_{ann} = 550$  °C, there is a phase transition at 766 °C, near to the Curie temperature  $T_C$  of pure bulk iron,  $T_C = 770$  °C. The transition temperature and the susceptibility drop at this temperature both increase with  $T_{ann}$ . This type of behavior has been observed in other systems<sup>31</sup>.

Figure 5a shows the remanence  $M_r$  as a function of annealing temperature.  $M_r$  decreases with increasing  $T_{ann}$ , despite a small peak at

**Table 1.** Average Fe particle sizes  $D_m$  in the Fe<sub>10</sub>Ag<sub>90</sub> granular alloy at different  $T_{ann}$  values.

$T_{ann}$ (°C)	400	450	500	550	600	700
$D_m$ (nm)	30.0	30.7	30.5	30.2	29.3	30.1



**Figure 3.** Room temperature hysteresis curves of the Fe<sub>10</sub>Ag<sub>90</sub> granular alloy samples for different annealing temperature. Insert: maximum field magnetization as a function of  $T_{ann}$ .

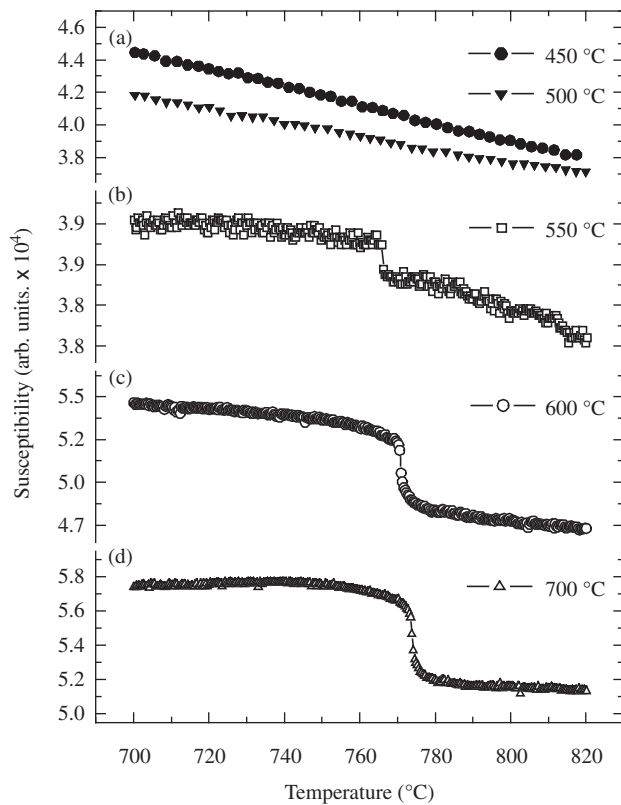


**Figure 4.** AC susceptibility of the Fe<sub>10</sub>Ag<sub>90</sub> granular alloy samples at different  $T_{\text{ann}}$ : a) 450 and 500 °C; b) 550 °C; c) 600 °C; and d) 700 °C.

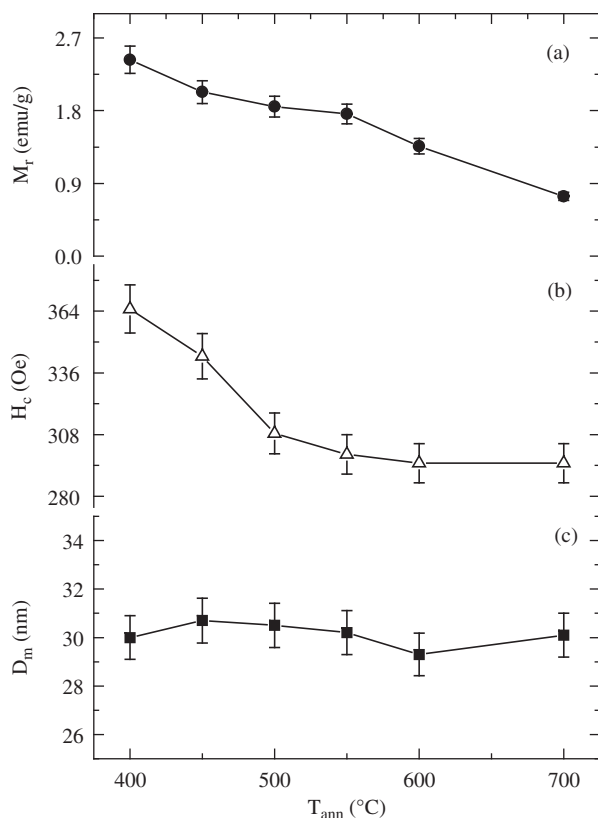


**Figure 5.** Magnetic properties of Fe<sub>10</sub>Ag<sub>90</sub> prepared at different annealing temperature. a) Remanent magnetization; b) Coercive field; and c) Fe mean particle diameter obtained from X-ray diffraction.

550 °C, as seen in hysteresis curves. Figure 5b shows the coercive field  $H_c$  vs.  $T_{\text{ann}}$ . One can see that  $H_c$  decreases significantly with increasing of  $T_{\text{ann}}$ , reaching a steady value of 295 Oe at  $T_{\text{ann}} = 600$  °C. This saturation in coercivity is probably due to the fact that for  $T_{\text{ann}} = 600$  °C there is a large number of bulk-like particles, as observed through the AC susceptibility curves (seen Figure 4). Another important observation may be made by comparing the coercive field with the average Fe grain size, displayed in Figure 5c, as a function of  $T_{\text{ann}}$ . We see that while  $H_c$  change significantly with  $T_{\text{ann}}$ ,  $D_m$  stays almost constant at around  $30 \pm 0.7$  nm. Thus, there is not a correlation between  $H_c$  and  $D_m$ , as there is in a non-interchange uniform particle system. However, in these samples there is a distribution of particle size. Both BL and SPM particles are present simultaneously, as confirmed by Mössbauer effect and magnetization measurements at room temperature<sup>28</sup>, even though the critical diameter of Fe spherical particle is 16 nm<sup>32</sup>, i.e. much less than  $D_m$ . Thus, heat treatment mainly modifies the distribution of particle sizes, and consequently the coercive field, which is a sum of contributions of all Fe particles in samples.

#### 4. Conclusions

Samples of Fe<sub>10</sub>Ag<sub>90</sub> granular alloys were thermally treated at various temperatures. Magnetic measurements show the existence of a distribution of particle sizes in these samples, which are composed of both SPM and BL particles. The magnetic properties of the samples are strongly influenced by changes in annealing temperature. For the samples annealed above of 550 °C appears a multidomain phase similar the  $\alpha$ -Fe phase, that was attributed to a process of atomic diffusion between the grains of Fe.

#### Acknowledgments

This work was partially supported by the Brazilian agencies CNPq, FINEP and CAPES.

#### References

- Henglein A. Small-particle research – physicochemical properties of extremely small colloidal metal and semiconductor particles. *Chemical Reviews*. 1989; 89(8):1861-1873.
- Greenblatt M. Molybdenum oxide bronzes with quasi-low-dimensional properties. *Chemical Reviews*. 1988; 88(1):31-53.
- Moffitt M, Eisenberg A. Size control of nanoparticles in semiconductor-polymer composites .I. Control via multiplet aggregation numbers in styrene-based random ionomers. *Chemistry of Materials*. 1995; 7(6):1178-1184.
- Ghosh K, Maiti SN. Mechanical properties of silver-powder-filled polypropylene composites. *Journal of Applied Polymer Science*. 1996; 60(3):323-331.
- Andres RP, Bielefeld JD, Henderson JI, Janes DB, Kolagunta VR, Kubiak CP, Mahoney WJ, Osifchin RJ. Self-assembly of a two-dimensional superlattice of molecularly linked metal clusters. *Science*. 1996; 273(5282):1690-1693.
- Forster S, Antonietti M. Amphiphilic block copolymers in structure-controlled nanomaterial hybrids. *Advanced Materials*. 1998; 10(3):195.
- Berkowitz AE, Mitchell JR, Carey MJ, Young AP, Zhang S, Spada FE, Parker FT, Hutten A, Thomas G. Giant magnetoresistance in heterogeneous Cu-Co alloys. *Physical Review Letters*. 1992; 68(25):3745-3748.
- Xiao JQ, Jiang JS, Chien CL. Giant magnetoresistance in nonmultilayer magnetic systems. *Physical Review Letters*. 1992; 68(25):3749-3752.
- Soares JM, de Araújo JH, Cabral FAO, Dumelow T, Machado FLA, de Araújo AEP. Giant magnetoimpedance in FeAg granular alloys. *Applied Physics Letters*. 2002; 80(14):2532-2534.
- Abeles B, Sheng P, Counts MD, Arie Y. Structural and electrical properties of granular metal-films. *Advanced Physics*. 1975; 24(3):407-461.

11. Abeles B. *Applied Solid State Science: Advances in Materials and Device Research*. New York: Academic Press; 1976.
12. Chen, C.I. Granular Magnetic Solids (Invited). *Journal of Applied Physics*. 1991; 69(8):5267-5272.
13. Kneller EF, Magnetic + structural properties of metastable Fe-Cu solid solutions. *Journal of Applied Physics*. 1964; 35(7):2210.
14. Korn D, Pfeifle H, Niebuhr J. Electrical-resistivity of metastable copper-iron solid-solutions. *Zeitschrift für Physik B-Condensed Matter*. 1976; 23(1):23-26.
15. Kajzar F, Parette G. Magnetic-moment distribution in bcc Fe-Cu alloys. *Journal of Applied Physics*. 1979; 50(3):1966-1968.
16. Longworth G, Jain R. Mossbauer-effect study of iron-implanted copper-alloys .1. As a function of dose. *Journal of Physics F-Metal Physics*. 1978; 8(2):351-362.
17. Sumiyama K, Nakamura Y, High-concentration Fe-Cu and Fe-Ag alloys produced by vapor quenching. *Physica Status Solidi A-Applied Research*. 1984; 81(2):K109-K112.
18. Sumiyama K, Yoshitake T, Nakamura Y. Thermal-stability of high-concentration Fe-Cu alloys produced by vapor quenching. *Acta Metallurgica*. 1985; 33(10):1785-1791.
19. Kataoka N, Sumiyama K, Nakamura Y. Magnetic-properties of high-concentration Fe-Ag alloys produced by vapor quenching. *Journal of Physics F-Metal Physics*. 1985; 15(6):1405-1411.
20. Sumiyama K, Kataoka N, Nakamura Y. Effect of Ar gas-pressure on structure and magnetic-properties of sputter-deposited Fe-Ag alloys. *Japanese Journal of Applied Physics*. 1988; 27(9):1693-1698.
21. Crespo-Sosa A, Schaaf P, Bolse W, Lieb KP, Gimbel M, Geyer U, Tosello C. Irradiation effects in Ag-Fe bilayers: Ion-beam mixing, recrystallization, and surface roughening. *Physical Review B*. 1996; 53(22):14795-14805.
22. Pankhurst QA, Cohen NS, Odlyha M. Thermal analysis of metastable Fe-Cu-Ag prepared by mechanical alloying. *Journal of Physics-Condensed Matter*. 1998; 10(7):1665-1676.
23. Mazzone G, Antisari MV. Structural and magnetic properties of metastable fcc Cu-Fe alloys. *Physical Review B*. 1996; 54(1):441-446.
24. Gómez JA, Xia SK, Passamani EC, Giordanengo B, Baggio-Saitovitch EM. Magnetic and magnetotransport properties of nanocrystalline Ag<sub>0.85</sub>Fe<sub>0.15</sub> and Ag<sub>0.70</sub>Fe<sub>0.30</sub> alloys prepared by mechanical alloying. *Journal of Magnetism and Magnetic Materials*. 2001; 223(2):112-118.
25. Lin HM, Tung CY, Yao YD, Hwu Y, Tsai WL, Tzeng SJ, Lin CK, Lee PY. Magnetic and structural properties of nanophase Ag<sub>x</sub>Fe<sub>1-x</sub> solid solution particles. *Nanostructured Materials*. 1998; 10(3):457-464.
26. Chatterjee A, Datta A, Giri AK, Das D, Chakravorty D. Iron nanoparticles in copper matrix prepared by sol-gel route. *Journal of Applied Physics*. 1992; 72(8):3832-3834.
27. Wang JP, Luo HL, Gao NF, Liu YY. The preparation and magnetic properties of Fe-Ag granular solid using a sol-gel method. *Journal of Materials Science*. 1996; 31(3):727-730.
28. Soares JM, de Araújo JH, Cabral FAO, de Araújo JAP, Sasaki JM. Preparation and characterization of FeAg granular alloys. *Materials Research*. 2004; 7(3):513-516.
29. Soares JM, de Araújo JH, Cabral FAO, Dumelow T, Xavier Jr MM, Sasaki JM. Size Distribution with Superparamagnetic and Blocked Particles in FeAg Granular Alloy. *Anais do 3o ENCONTRO DA SBPMat*, Symposium A, 2000 Foz do Iguaçu, Brasil, v. 1, 2000. p. 70.
30. de Moraes E. *Estudo da oxigenação dos compostos intermetálicos Fe<sub>17</sub>r<sub>2</sub> (R=SM, PR, ND)*. [Ph.D thesis]. Campinas: Instituto de Física "Gleb Wataghin", Unicamp; 1999.
31. Nepijko SA, Wiesendanger R. Size dependence of the Curie-temperature of separate nickel particles studied by interference electron-microscopy. *Europhysics Letters*. 1995; 31(9):567-572.
32. Cullity BD. *Introduction to Magnetic Materials*. Reading, MA: Addison-Wesley; 1972.